ASSESSING EMBRYONIC TOXICITY AND END FATES OF NANOPLASTICS IN FRESHWATER ENVIRONMENTS USING GASTROPOD *BIOMPHALARIA GLABRATA*

A Thesis

by

MACKENZIE L. MERRILL

BS, Texas A&M University at Galveston, 2017

Submitted in Partial Fulfillment of the Requirements for the Degree of

MASTER OF SCIENCE

in

BIOLOGY

Texas A&M University-Corpus Christi
Corpus Christi, Texas

August 2022

August 2022

ASSESSING EMBRYONIC TOXICITY AND END FATES OF NANOPLASTICS IN FRESHWATER ENVIRONMENTS USING GASTROPOD *BIOMPHALARIA GLABRATA*

A Thesis

by

MACKENZIE L. MERRILL

This thesis meets the standards for scope and quality of
Texas A&M University-Corpus Christi and is hereby approved.

Wei Xu, Ph.D.
Chair

Keisha Bahr, Ph.D.
Committee Member

Daniel Wagner, Ph.D.
Committee Member

Riccardo Mozzachiodi, Ph.D.
Committee Member

August 2022

ABSTRACT

The wide use of plastics has resulted in not only the accumulation of macroplastic pollution in the aquatic environment but also plastic particles at micro and nano levels (MPs and NPs). Accumulation of these MPs and NPs have numerous adverse effects on the morphology, behavior, and reproduction of living organisms. In this study, we investigated the effects of NPs on the embryonic development of *Biomphalaria glabrata*, a commonly used gastropod in toxicology studies. This study identified the adsorption of NPs by the embryos of *B. glabrata* and showed evidence of NP absorption by the hatched juveniles. NP bioaccumulation subsequently triggered the alteration in the expression of several stress response genes, including heat shock protein-70 (HSP70), cytochrome P450 (CYP450), and macrophage migration inhibitory factor (MIF). With the influence of NPs, the hatching rates of *B. glabrata* embryos varied depending on the sizes of NPs. In addition, the NPs with mean diameters of 1.0 μm or 0.03 μm led to higher embryo mortality rates than 0.5 μm NPs. This preliminary study demonstrated the impact of NPs on the development of *B. glabrata* embryos. Further studies on the mechanism of NP toxic effects are desired.

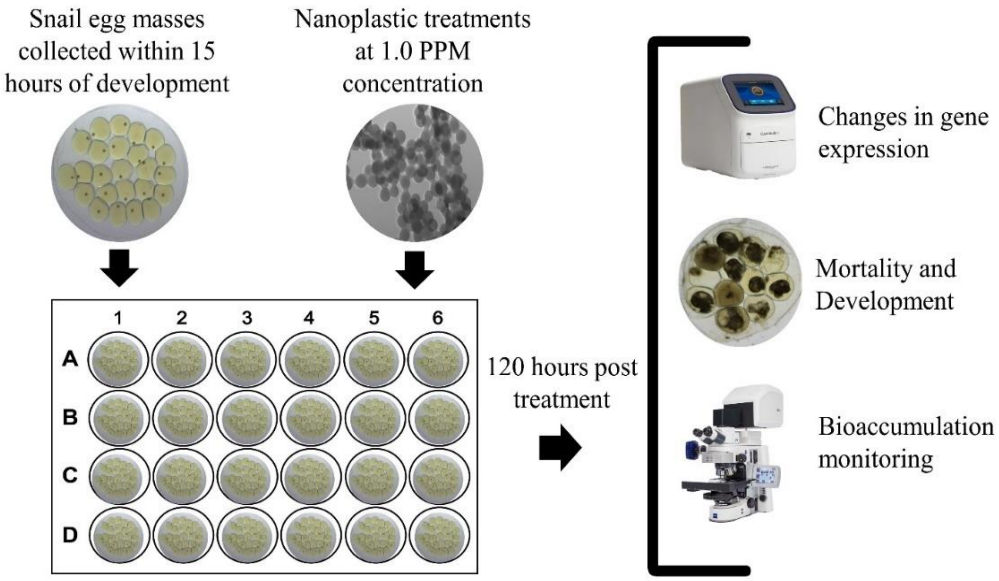

Figure 1: Graphical representation of abstract.

DEDICATION

To my husband for getting me through.

ACKNOWLEDGEMENTS

Thank you to my PI, Dr. Wei Xu, for the opportunity to continue my education and betterment as a scientist and for his mentorship throughout my master's career. I also want to thank my committee members, Dr. Keisha Bahr, Dr. Riccardo Mozzachiodi, and Dr. Dan Wagner, for their guidance and support during this process. Thank you to Dr. Wagner for providing the lab with *B. glabrata* individuals to start our research population. Finally, thank you to all my lab members: Dr. Leisha Martin, Sandra Marbach, Molly Brzezinski, Nin Gan, Kayla Simpson, Chi Huang, Carley Armendarez, and Kaitlin Garcia for their endless help and encouragement.

TABLE OF CONTENTS

PAGE

LIST OF FIGURES

Page

LIST OF TABLES

Page

1. INTRODUCTION

Plastic Pollution

While microplastics have become a widely recognized issue facing the environment, the recognition of micro and nano-sized plastics has been met with increasing concern from the scientific community (Koelmans *et al*., 2015). Approximately eight billion tons of plastic waste are estimated to enter oceans annually, and roughly 80% of microplastic in the ocean is from land-based sources (Jambeck *et al*., 2015; Rochman, 2018). Tons of manufactured micro/nanoplastics (MNPs) enter environments through anthropological wastewater effluent as they cannot be efficiently removed from wastewater treatment systems (Murphy *et al*., 2016), or they are generated from the degradation of macroplastics via photolysis, oxidization, and biological metabolization (Eubeler *et al*., 2009). Although some larger plastic particles can be removed from wastewater, the removal efficacy is low for smaller particles (10-300 μm) (Browne *et al*., 2011). The estimated concentration of the microplastics discharged into the water is around 0.25 mg/L (Murphy *et al*., 2016). These microplastic particles accumulate in freshwaters and can result in higher concentrations over time.

The degradation of plastics also contributes to the increasing concentration of MNPs in the environment. Once plastics enter the environment, they become brittle through chemical, physical, and biological processes, collectively termed weathering (Eubeler *et al*., 2009). Over time, weathering of these plastic pieces degrades them into various sizes of plastic particles, including microplastics (1 μm - 5mm) and nanoplastics (Lambert & Wagner, 2016). There is no consensus in the literature regarding the classification of nanoplastics to a specific size range. However, they are often described as plastic (synthetic polymeric) particles ranging from 0.1 μm to 1.0 μm in diameter (da Costa *et al*., 2018; Lehner *et al*., 2019), whereas The National Science Foundation

defines nanoplastic as particles under 0.1 µm. Recent studies reported the degradation of several types of plastics under simulated environmental conditions. One study demonstrated the weathered polyethylene (PE) microplastics which showed microcracking in eight weeks, and another degraded polystyrene (PS) which saw the formation of nanoparticles (NPs) in four weeks (da Costa *et al*., 2018; Lambert & Wagner, 2016).

One of the most pressing issues surrounding micro and nanoplastics is the lack of data regarding the environmental distribution. Without the availability of data quantifying current environmental concentrations, it is difficult to accurately assess ecological health impacts (Bouwmeester *et al*., 2015). Other urgent topics meriting further investigation include MNP end fates in the environment, trophic transfer, effects of chronic exposure, and potential transgenerational effects for a more comprehensive understanding of MNP risk in aquatic environments (Chae *et al.*, 2017; Lehner *et al*., 2019). Lastly, the toxicity of MNPs in freshwater environments has been grossly under-investigated compared to marine environments (Chae *et al*., 2017), though research has collectively demonstrated that MNPs toxicity is dependent on multiple factors, including environmental conditions and species (Tosetto *et al*., 2016; Kashiwada, 2006); Rainieri *et al*., 2018; Green *et al.*, 2016; Kögel *et al*., 2020).

Nanoplastic Toxicity to Aquatic Organisms

Numerous studies have shown that NPs at various concentrations have the potential to inhibit adult growth, alter normal development, modify behavior, and decrease survival rates in aquatic organisms (Balbi *et al*., 2017; Cui *et al*., 2017; Lee *et al*., 2013; Pitt *et al*., 2018). Due to the small size, NPs may also cross biological membranes, causing adverse effects on a cellular scale (Sökmen *et al*., 2020). Studies have shown that NPs interact differently within the environment when compared with MPs composed of the same material. This finding has revealed

the need for additional research, specifically on nanoplastic interactions in diverse environments and organisms (Maurer-Jones *et al*., 2013; Zhang & Coultas, 2011).

Another factor to consider is the sedimentation of these NPs, due to the density of the particles, agglomeration, and the occurrence of biofouling (Cole *et al*., 2016; Lagarde *et al*., 2016; Long *et al*., 2015; Martin *et al*., 2017; van Cauwenberghe *et al*., 2013) Thus, bottom feeders are unique because their ecological niche increases their potential to interact with MNPs in aquatic environments through absorption and ingestion, putting them at higher risk for nanoplastic bioaccumulation and therefore increasing the potential for transfer to higher trophic levels (Liu *et al*., 2014; Luo *et al*., 2015).

Research Model *Biomphalaria glabrata*

Invertebrate species are frequently used to biomonitor water quality due to their sensitivity to environmental disturbances (Besseling *et al*., 2014; Browne *et al*., 2008; Oliveira-Filho *et al*., 2016; Tallec *et al*., 2018) *Biomphalaria glabrata* (Mollusca, Gastropoda), commonly known as a blood fluke planorb, is a freshwater pulmonated, hermaphroditic snail species commonly used in toxicological studies (Caixeta *et al*., 2021; Tallarico, 2015; Lima *et al*., 2019; Oliveira-Filho *et al*., 2016, 2017, and 2019). They typically live in shallow water and are generalist herbivores that feed on the detritus of freshwater ecosystems by scraping or cutting the bottom substrate with their radula (Thomas *et al*., 1985)

The genome of *B. glabrata* has been sequenced and annotated (Hillier *et al*., 2017) due to their interest in human health parasitology studies. In research of environmental toxicology, *B. glabrata* demonstrated high sensitivity to nanoscale pollutants (i.e., metals, Ag, γ-Fe_2O_3, iron oxide nanoparticles, and cadmium telluride quantum dots) (Caixeta *et al*., 2021; Lima *et al*., 2019; Tallarico, 2015; Oliveira-Filho *et al*., 2016 and 2019). Furthermore, studies that have employed B.

glabrata to investigate nanoparticle ecotoxicity have identified reproductive and developmental biomarkers (Caixeta *et al*., 2021; Oliveira-Filho *et al*., 2016, and 2019). They are also small, cost-efficient, and require low maintenance in a laboratory setting. This model has yet to be utilized to study MNPs pollution.

The lifespan of *B. glabrata* is short. In laboratory conditions, they often do not live past 12 months, and the embryos develop within six to eight days (Pimentel, 1957; Toledo & Fried, 2011). The early embryonic development of *B. glabrata* follows the pattern of spiral holoblastic cleavage as the most common cleavage method employed by most mollusk embryos. Egg masses are translucent yellow-brown with an outer protective membrane surrounding an average of twenty egg capsules per mass, allowing clear visualization of development, which can be seen in Figure 2.

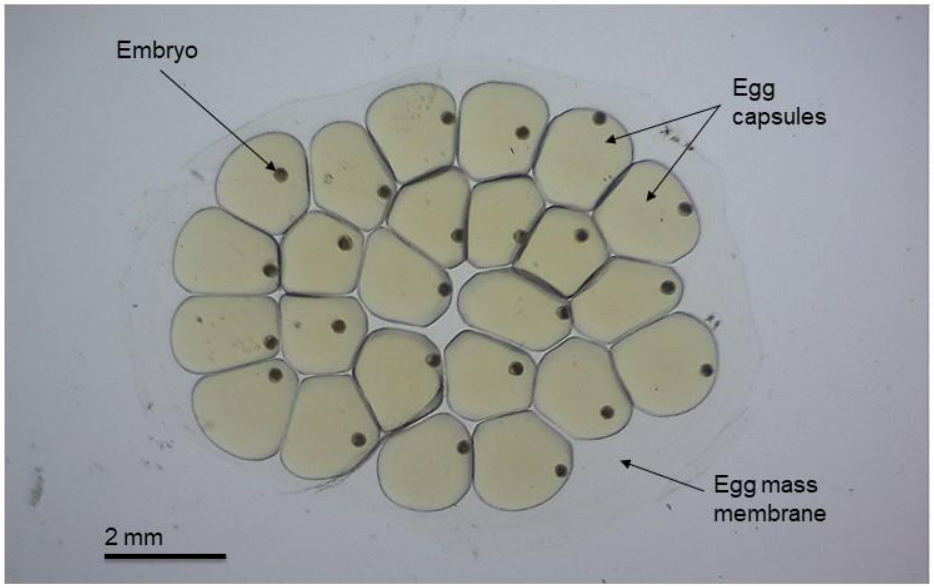

Figure 2: Single B. glabrata egg mass with 24 eggs encapsulated by an outer membrane, with embryos in the blastula phase of development (~15 hours old).

In an average of eight days, juveniles typically emerge less than 1.0 mm in diameter and are sexually mature within eight to ten weeks, and are roughly 10 to 11 mm in diameter (Pimentel, 1957). *Biomphalaria glabrata* is a promising species to study toxicological effects over ontogeny and generationally due to their life history and ecology (Tallarico, 2015; Oliveira-Filho *et al*., 2017). In laboratory conditions, the average survival longevity is 12 to 24 months, and snails can produce as many as 10,000 eggs per year. Their development within the egg takes roughly six to eight days and matures within ten weeks (Pimentel, 1957). Snails mature and begin oviposition between sizes ranging from 6.9 mm to 10.5 mm, which takes an average of 10 weeks to obtain (Pimentel, 1957). At this size range, snails typically produce 0-8 eggs per week with 2 – 31 eggs per mass, and as snails age, their fecundity and eggs per mass increase (Pimentel, 1957). This presents an exciting opportunity to study nanoplastic ecotoxicity using a gastropod model that also shows potential for being used as a biomonitoring tool for nanoparticle pollution in freshwater environments.

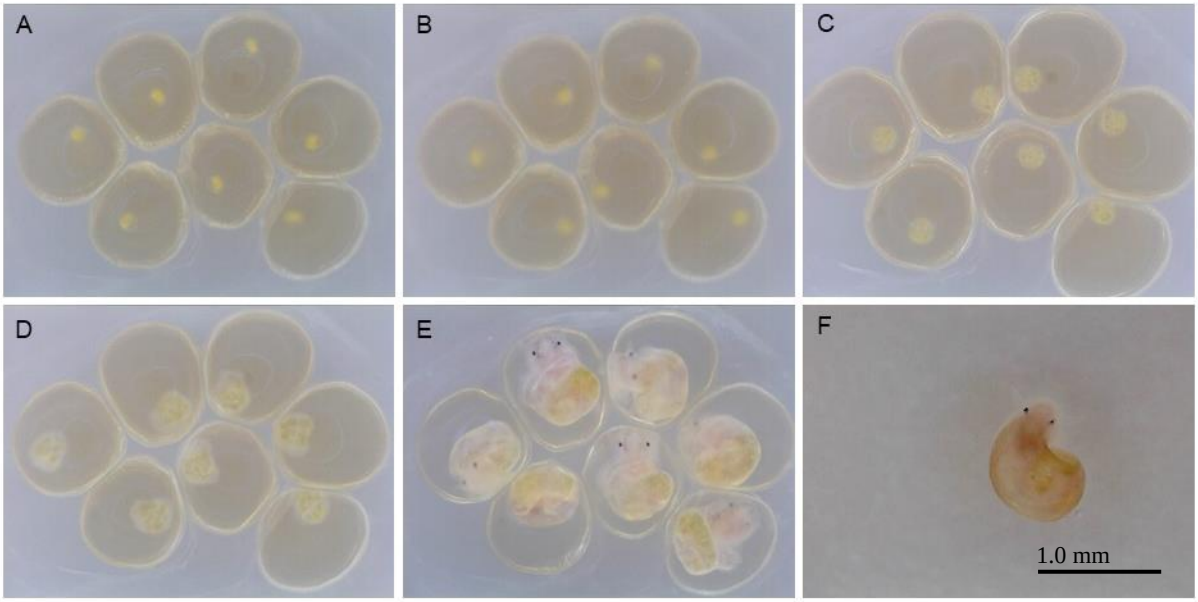

Figure 3: Early development stages of B. glabrata. (A) Blastula (15 hours post spawning, hps), (B) gastulae (26 hps), (C) trochophore (43 hps), (D) veliger (96 hps), (E) hippo-stage (120 hps), and (F) a newly hatched snail (144 hps).

Objectives and Hypothesis

This study aimed to investigate 1) the pathogenic pathways of NPs using *B. glabrata*, 2) toxicity and genetic response during embryonic development, and 3) the effects on embryonic mortality and hatching. It is hypothesized that the polystyrene nanoplastic particles below a specific size will be accumulated in the embryos of *B. glabrata* and result in the alteration in embryonic development as well as the genetic responses of the embryos. The protocols developed under this study will also provide a reference for the use of *B. glabrata* as an indicator for ecotoxicology studies.

2. MATERIALS AND METHODS

Nanoplastic Characterization and Preparation

Three sizes of PNPs that were used are 0.03 µm, 0.5 µm, and 1.0 µm, at 1.0 ppm concentrations. The PNPs used were fluorescently tagged, spherical latex beads with carboxylate-modified polystyrene in aqueous suspension purchased from Sigma Aldrich, St. Louis, MO (Product Number: 0.03 µm -L5155, 0.5 µm – L2380, 1.0 µm – L4655). The PNP stocking solutions came in concentrations of 25,000 ppm, which were then diluted with "snail water" to make 1.0 ppm concentration treatments. See "Study Animals" for the snail water description. Treatments were stored at 26°C in 25 mL falcon tubes wrapped in tin foil and thoroughly resuspended to ensure homogeneity of treatment before using again. Control treatments consisted of filtered snail water, the same as what the adults are reared in.

Study Animals

Fifteen four-month-old pigmented individuals between 8.0 and 12.0 mm in shell diameter, weighing between 0.24 g and 0.32 g, were used as egg producers for egg collections. Pigmented individuals were used for consistency and were chosen over unpigmented because they made up a larger portion of the housed population. The fifteen *B. glabrata* individuals (BB02 strain) were reared from a breeding stock obtained from the Department of Bioscience at Rice University. BB02 (*Biomphalaria* from Barreiro caught in 2002) strain was generated from field isolates in Brazil, and their genomic DNA was used as the template to produce the BAC (Bacterial Artificial Chromosome) library or a Bacterial Artificial Chromosome library, which stores fragments of DNA for simpler sequencing. Snails were reared in laboratory conditions in two-quart (7×11 in.) Pyrex pans filled with 1.0 L of filtered snail water. Tanks were stored in an incubator set to 26°C with alternating 12-hour light and dark cycles. Snail water was made by mixing 0.5 g of reef

crystals instant ocean and 1.0 g of sodium bicarbonate in 5.0 L of reverse osmosis (RO) water overnight. Before use, mixed snail water was filtered using a 1 L, 0.2 µm polyethersulfone (PES) membrane vacuum filter. Snails were fed a diet of spinach and green leaf lettuce, which was changed every other day. Each Pyrex pan held 15 individual animals, fecal matter was removed every two days using an electric pipette, and fresh snail water was added to maintain water levels at 1.0 L per tank.

Experimental Design

In the wild egg, masses were laid on a hard substrate or submerged vegetation, while in the laboratory, they preferred to lay on Styrofoam, glass walls, lettuce, or the shells of others. Styrofoam floats were placed in tanks overnight for snails to lay their embryos on and collected 15 hours later, while still in the blastula stage of development, to start treatment. Egg masses were carefully removed and inspected for any damage or abnormalities before being placed in a 24-well plate and randomly assigned a treatment. All excess water was removed before adding 2 mL of either aqueous PNP solution for the treatment groups or filtered snail water for the control groups to each well. Eggs were incubated at 26 °C with 12-hour light and dark cycles for the next 144 hours (6 days) and only removed for brief monitoring every 24 hours.

Florescent Quantification Assays

To estimate the total amount of PNP accumulation in the egg mass, PNPs left in the water after each day of treatment were quantified using a Cytation5 photospectrometry-based plate reader (BioTek Instruments, Winooski, VT). First, a standard curve was created using three known NP concentrations of 0.1, 1.0, and 10 ppm, which was used to normalize the data showing the changes in fluorescent intensity over the treatment duration. Standard curves were made for each of the NP sizes of 0.03, 0.5, and 1.0 µm. Embryos were cultured in their respective treatments for

six days, the entire embryonic development period, and a 100 μL water sample was taken from the same well every 24 hours for the six-day treatment duration. This experiment had three replicates for each treatment at each time point (n=3). Water samples were stored in a microcentrifuge tube wrapped in paraffin and stored at 4°C until ready for processing. Water samples were added to a 96-well plate, and the intensity of the fluorescent signal was quantified using the Cytation5 (BioTek Instruments, Winooski, VT) plate reader. The 0.03 μm and 1.0 μm yellow-green fluorescent PNPs have an emission wavelength of 505 nm with an excitation wavelength of 470 nm. The emission wavelength for the red 0.05 μm PNPs is 540nm with an excitation wavelength of 475 nm. Fluorescent intensity readings of the treatments were normalized with the respective blank average of each treatment.

Nanoplastic Bioaccumulation

Qualitative fluorescent imaging was used to visualize the accumulation and uptake of PNPs over the five-day treatment period. Eggs were collected within 15 HPS and randomly assigned a treatment. A standard inverted microscope (Olympus Co., Tokyo, Japan) equipped with a mercury lamp and a CCD camera was used to monitor the accumulation of the fluorescent PNP's on the surface of the egg mass and hatched juveniles for potential PNPs in their shell and or soft tissues. An egg mass from each treatment group and control group was collected every 24 hours post-treatment (HPT) and sacrificed to be imaged. To avoid fluorescent bleaching in our imaging results, egg masses were not used again after being exposed to the mercury lamp during imaging. Egg masses collected for imaging were gently removed from the well and rinsed with control snail water to wash off any NPs that were only sitting on the surface and were not imaged in treatment water. After 72 (HPT), eggs were also temperature shocked in a small amount of control water at 4°C for 10 – 20 minutes, depending on the developmental stage, to reduce the movement. Snail

movement within the egg capsule after 72 HPS begins to compromise the integrity of the fluorescent image. This method of temperature shocking the egg mass to reduce embryonic movement for fluorescent imaging was developed during this study. To monitor hatched juveniles for NPs, at 120 HPT, egg masses were carefully removed from treatment water, rinsed, and placed into a new well with control water for the snails to hatch. This was to ensure NP in the water and sitting on the surface of the egg mass would not accumulate on the juvenile as it emerges.

Gene Expression Analysis

Four egg masses from treatment groups and control groups were collected in 500 µL of TRIzol reagent and stored at -80 °C for use in gene expression analysis. RNA extractions were performed following standard extraction and purification procedures (Toni *et al.,* 2018). After RNA extraction was complete, the purity and quality (260/280 nm values) of each sample were evaluated, and RNA was quantified in ng/µL using the Eppendorf BioSpectrometer (Eppendorf Biotech, Hamburg, Germany). The average ratio of the 260/280 nm values was 1.5. RNA samples of sufficient quality were diluted in molecular water for cDNA synthesis, which was performed using the Invitrogen SuperScript IV reverse transcription system with a random hexamer primer (Invitrogen Co., Carlsbad, CA). Samples were processed in the Thermocycler (Thermo Fisher Scientific, Waltham, MA) according to the predetermined timeline for the SuperScript IV transcription kit, and the cDNA products were stored at -20°C for downstream processing. Within literature n=3 is a common sample size, though for this study n=4 was used as means to potentially increase the validity and normality of the data.

The relative gene expression of five known genes relating to xenobiotic, environmental stress, and innate immune responses was quantified by quantitative PCR (qPCR) using the Thermo Fisher QuantStudio 3 (Thermo Fisher Scientific, Waltham, MA) qPCR instrument. Genes were

Table 1: List and descriptions of B. Glabrata genes used in this study.

Target Gene	Protein Encoded	Primer Pair Sequence	Gene Description
GAPDH	Glyceraldehyde 3-phosphate dehydrogenase	F: 5'- TCT CCA CCT CCC TAC AGA AA –3' R: 5'- GGA AGT TGT CCG AAT GGA GTA T -3'	Reference Gene (Giusti *et al*., 2013)
HSP70	Heat Shock Protein-70	F: 5'-AAG AGA AGC ACC ACC ATT CC -3' R: 5'- CGA TGT CGA ATG TGA CCT CTA TC -3'	Environmental stress response (Song *et al.*, 2014)
CYP450	Cytochrome P450	F: 5'- CAG CAG ACA GGA AAG ACC TAAT -3' R: 5' CAC TTC GAC ACT GAC AGA TCC -3'	Xenobiotic stimuli response (Whalen *et al*., 2010)
MATN1	Matrilin-1	F: 5'- TCC GAG TCT CAA TCA TTA GC -3' R: 5' - CAT ATA CTG GAT GGC CCT -3'	Formation of tissues,; is expressed during B. glabrate embryonic development (Bouchut, 2006)
MIF	Macrophage Migration Inhibition Factor	F: 5'- TGC CAG CCC TGT TCT GTC A-3' R: 5' - TCC CTT GAG GTC TTA ATC AC -3'	Stress response (Garcia *et al*., 2010)

selected due to their use in previous animal ecology and ecotoxicology studies or their use in other experiments using *B. glabrata*. To test the relative gene expression changes between PNP treatment groups and control groups, Glyceraldehyde 3-phosphate dehydrogenase (GAPDH) was used as a reference gene to normalize the data of the following genes: cytochrome P450 (CYP32A1), heat shock protein 70 B2-like (HSP70), macrophage migration inhibition factor (MIF) and matrilin (MATN1). The primers for this study were designed through Integrated DNA Technologies' custom primers website (IDT, USA), using the available sequences from the NCBI

gene bank, which can be seen in Table 1. Primers were tested and confirmed using PCR and gel electrophoresis before being used for qPCR analysis. The delta-delta-CT or DDCT algorithm was used to analyze the relative changes in gene expression in comparison to the housekeeping gene.

Acute Toxicity Assay

Every 24 hours for five days (24, 48-, 72-, 96-, and 120 HPT egg masses (n=6) from each treatment were monitored under a stereomicroscope for embryo mortality rate (EM) and hatching rate (HR) (Caixeta *et at*., 2021). The EM (%) was calculated by dividing the number of dead embryos by the total number of embryos per clutch and then multiplying by 100 (Caixeta *et at*., 2021; OCED, 2016; Melo *et at.*, 2019). Deceased embryos were identified by lack of movement and heartbeat or if the embryo began to disintegrate (Oliveira *et at*., 2010). HR (%) was calculated by dividing the number of hatched snails by the total number of embryos per clutch and then multiplying by 100 (Caixeta *et at*., 2021; Melo *et at.*, 2019). The hatched snail had to have left the egg mass entirely and not just the egg capsule to be counted.

Statistical Analysis

Statistical analyses were conducted in Rstudio. Fluorescent quantification, hatching rate, mortality rate, and qPCR data were parametric; thus, a Shapiro–Wilk test was used to test for normality and was followed by one-way ANOVA for significance (p-value <0.05). The difference in treatment groups over each time point was evaluated using a Tukey's test.

3. RESULTS

Florescent Quantification Assays

The results of measuring the intensity of the NP's fluorescent intensity using photo spectrometry analysis of water samples showed fewer NPs were detected in the treatment water at the end of 120 hours compared to the starting treatment at 0 Hours across all treatments. A standard curve was created using three concentrations known concentrations of 0.1, 1.0, and 10.0 ppm for 0.03 µm NPs absorbed and the standard curve for 0.03 µm treatment fluorescence intensity readings with the trendline equation ($y = 484.61x – 250.32$; $R^2 = 0.9925$). Figure 5 shows the

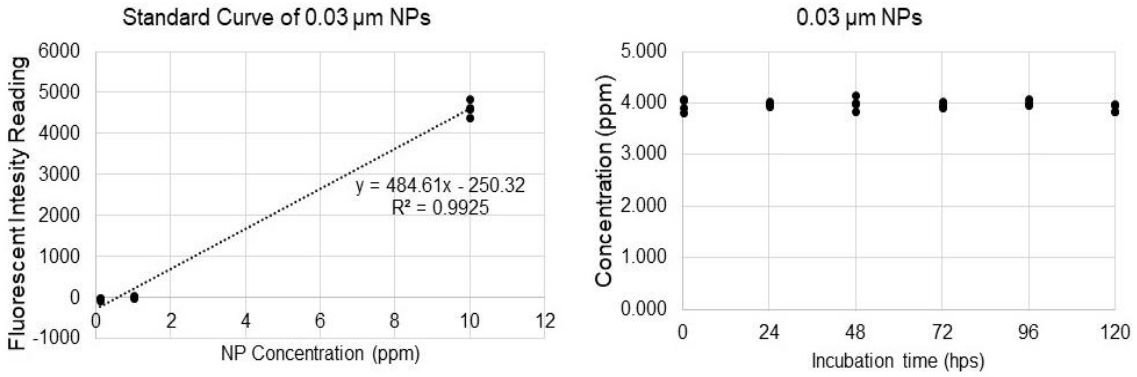

Figure 4: Estimation of NP 0.03 µm absorption by B. glabrata embryos (n=3).

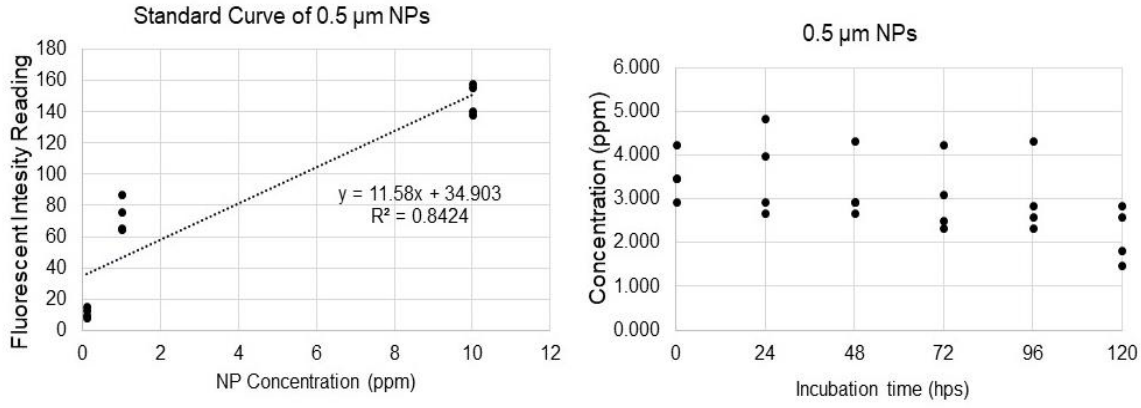

Figure 5: Estimation of NP 0.5 µm absorption by B. glabrata embryos (n=3).

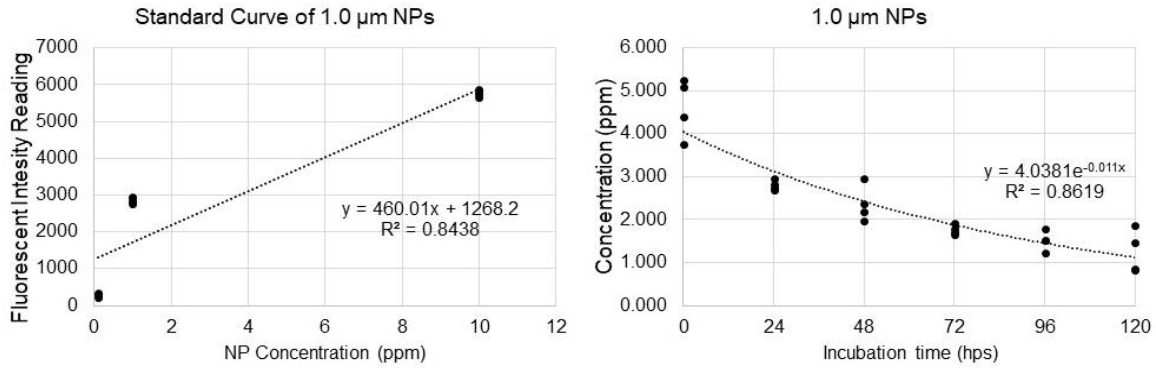

Figure 6: Estimation of NP 1.0 µm absorption by B. glabrata embryos (n=3).

estimation of 0.5 µm NPs absorbed and the standard curve for 0.5 µm treatment fluorescence intensity readings with the trendline equation ($y = 11.58x + 34.903$; $R^2 = 0.8424$). Figure 6 shows the estimation of 1.0 µm NPs absorbed the standard curve for 1.0 µm treatment fluorescence intensity readings with the trendline equation ($y = 460.01x + 1268.2$; $R^2 = 0.8438$).

Nanoplastic Bioaccumulation

Fluorescent imaging of egg masses exposed to fluorescently tagged PNPs showed bioaccumulation of PNPs on the surface of the egg masses across all three treatments (Figures 7-11). Though these images in Figures 7-10 could not serve as a clear indicator for PNP migration through the outer membrane and uptake by the embryo, increased NP density on the surface could be visualized by increased diameter of fluorescent signals. Colors to fluorescent images were added using image processing software (ImageJ). Figure 7 shows a visual comparison of the treatments over each 24-hour time point and how bioaccumulation of NP on the outer surface of the egg mass increases with exposure time.

Fluorescent images of treatment 0.03 µm at 24 HPT and 96 HPT can be seen in Figure 8. Treatment 0.03 µm had a single florescent signal at 24 HPT. At 96 HPT, many more NPs can be visualized as well as clusters of NPs which is suggested by the increased diameter of fluorescent

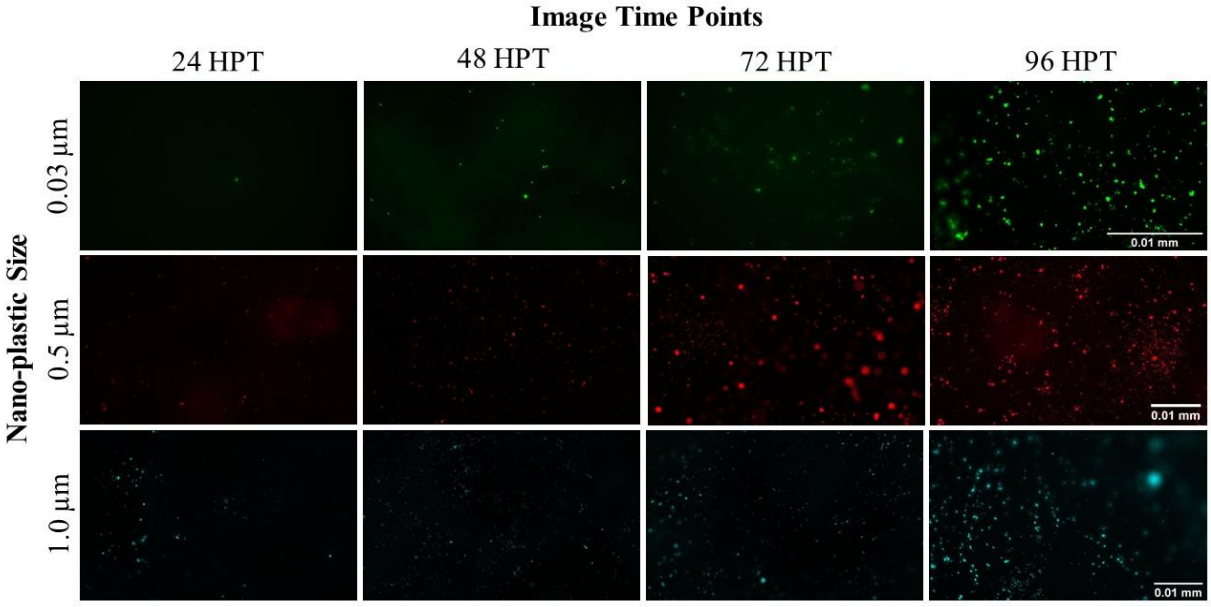

Figure 7: Flourescent image compairison of treatments over exposure time. Flourescent signals can be seen as early as 24 HPT and bioaccmulation increases over treatmenr

signals. The 0.03 µm NPs seemed to group with fewer signals seen between the larger glomerations. Fluorescent images of treatment 0.5 µm at 24 HPT and 96 HPT can be seen in Figure 9. Treatment 0.5 µm at 24 HPT was sparsely covered in NPs with a few clusters. By 96 HPT, there were many more clusters with many small signals in-between. Fluorescent images of treatment 1.0 µm at 24 HPT and 96 HPT can be seen in Figure 10. At 24 HPT treatment of 1.0 µm, the egg mass had only an area with clusters of NPs. At 96 HPT, much of the surface is covered in NPs and has larger clusters than seen in the previous treatments.

Fluorescent scanning using a standard, inverted microscope only allowed visualizing of NPs on the outside of the egg mass, but internal distribution was able to be detected by conducting a Z-scan on a Zeiss confocal scope (Figure 11). The Z-scan image showed that 0.03 µm PNPs at 10.0 ppm were able to penetrate the outer membrane. None of the 1.0 ppm treatments produced

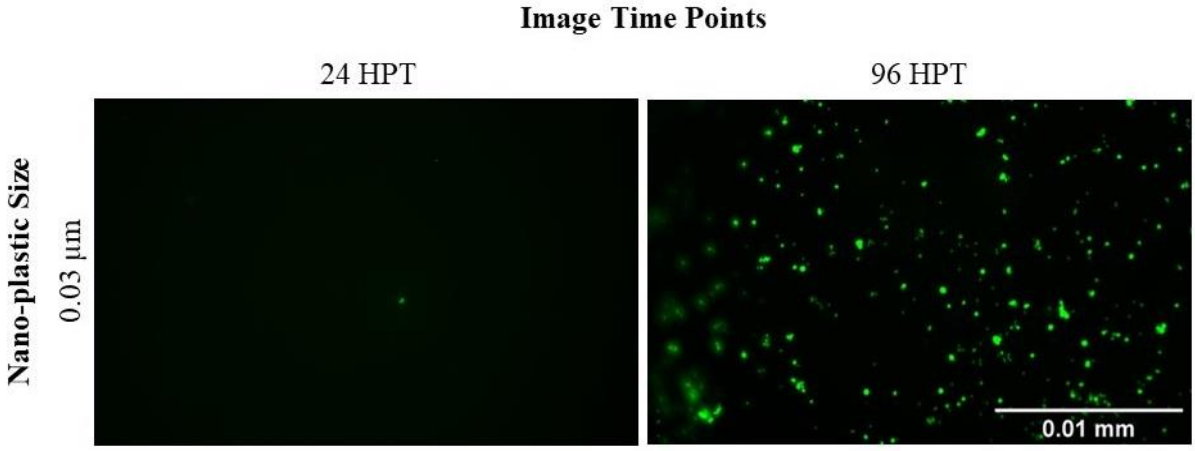

Figure 8: Flourescent images of treatment 0.03µm at 24 HPT and 96 HPT.

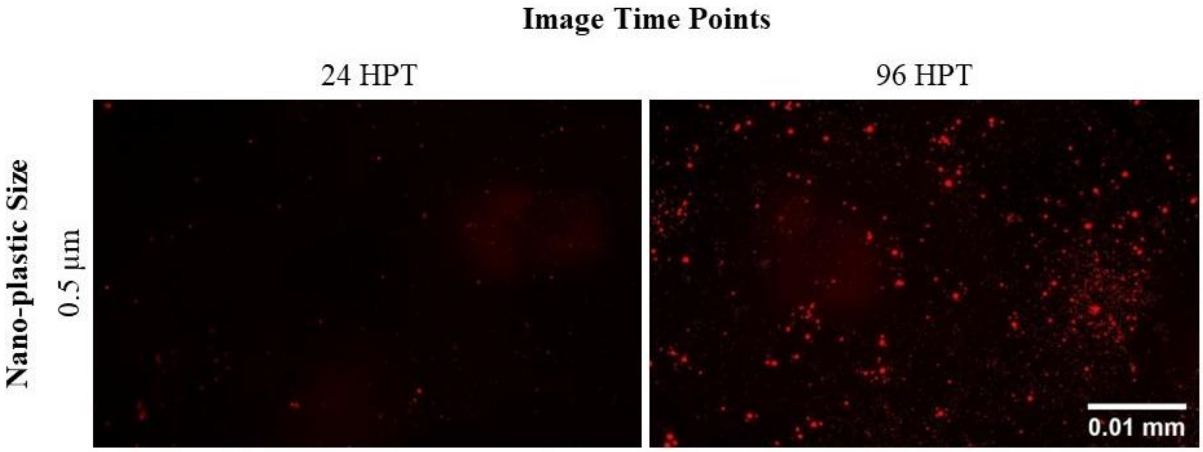

Figure 9: Flourescent images of treatment 0.5 µm at 24 HPT and 96 HPT.

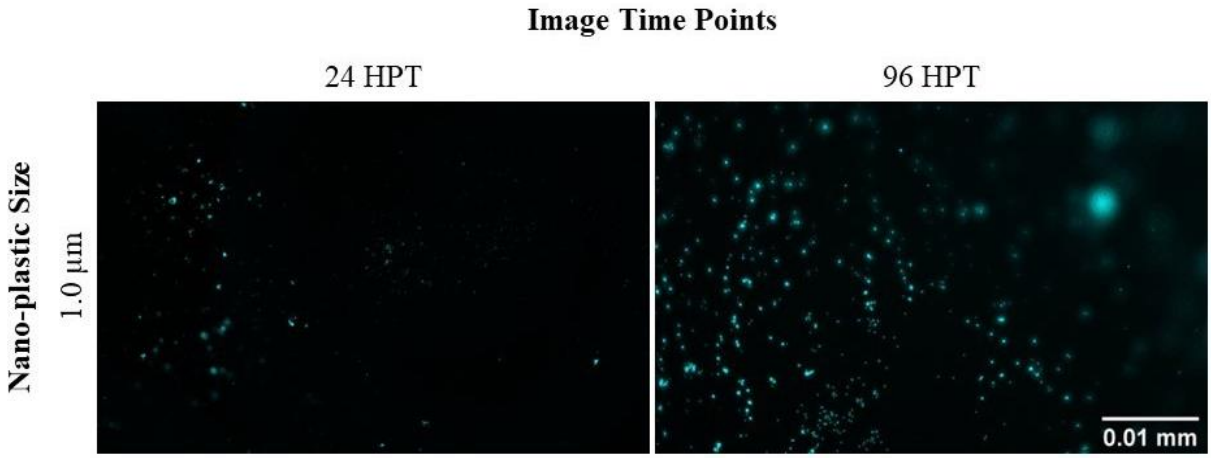

Figure 10: Flourescent images of treatment 1.0 µm at 24 HPT and 96 HPT.

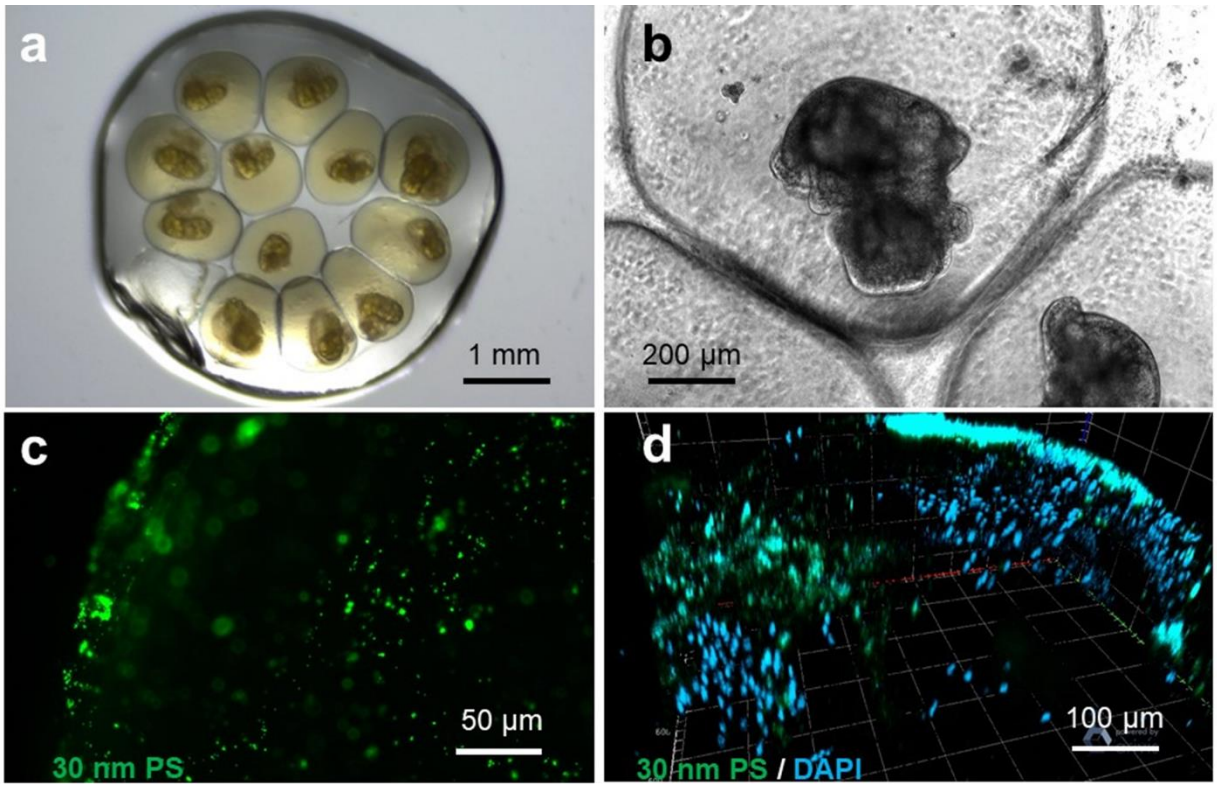

Figure 11: Imaging of fluorescent polystyrene in B. glabrata. Embryos of B. glabrata developed for 5 days (a and b) were treated with 0.03 µm fluorescent PNPs at 10.0 ppm. The fluorescent signals can be seen on the surface of the egg mass with a scanning fluorescent microscope (c), but the internal distribution of PNPs can only be detected by Z-scan with Zeiss confocal scope (d).

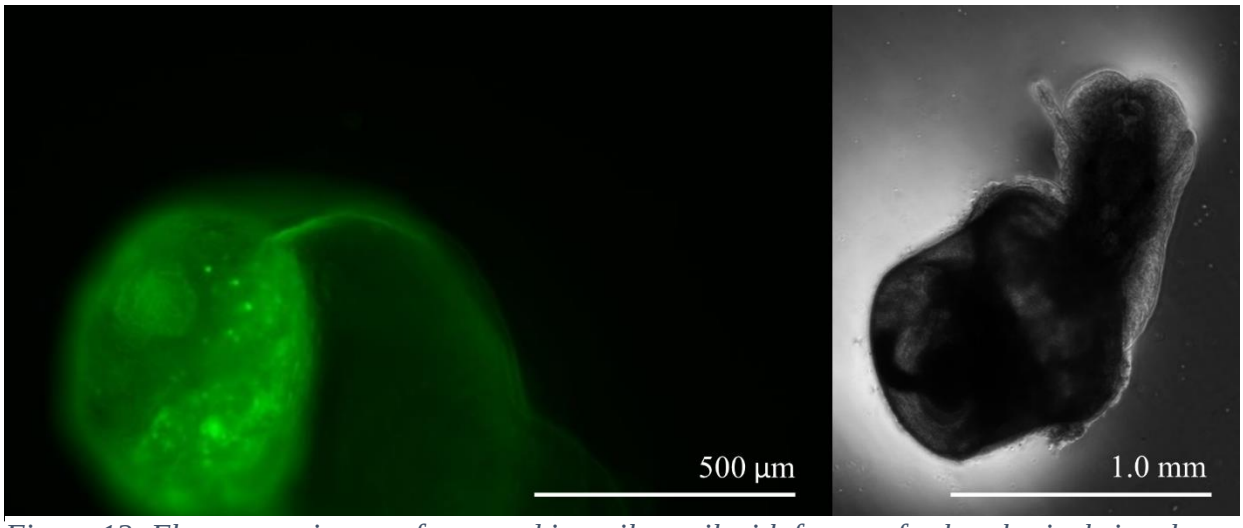

Figure 12: Fluorescent image of emerged juvenile snail with four perfectly spherical signals coming from the shell in the image to the left, and a brightfield image of the same juvenile on the right.

hatched juveniles with fluorescent signals. During a preliminary experiment, egg masses were exposed to the 0.03 µm NPs at 10.0 ppm and did see a hatched juvenile with what looked like fluorescent NP signals (Figure 12).

Relative Gene Expression Assays

Targeted gene expression was analyzed for stress response, xenobiotic, and innate immune responses and compared to the control values. Gene expression results for HSP70 showed variation in gene expression over development for treatment groups, while the control values stayed relatively similar, as seen in Figure 13. In the figure below and the following, error bars represent the mean of the standard deviation. At 48 HPT for treatment 0.03 µm was significantly upregulated with a fold change difference of 0.2 from the control, 0.6 from 1.0 µm and 0.9 from 0.5 µm (p-value <0.05). At 120 HPT the control treatment was significantly upregulated with a fold change

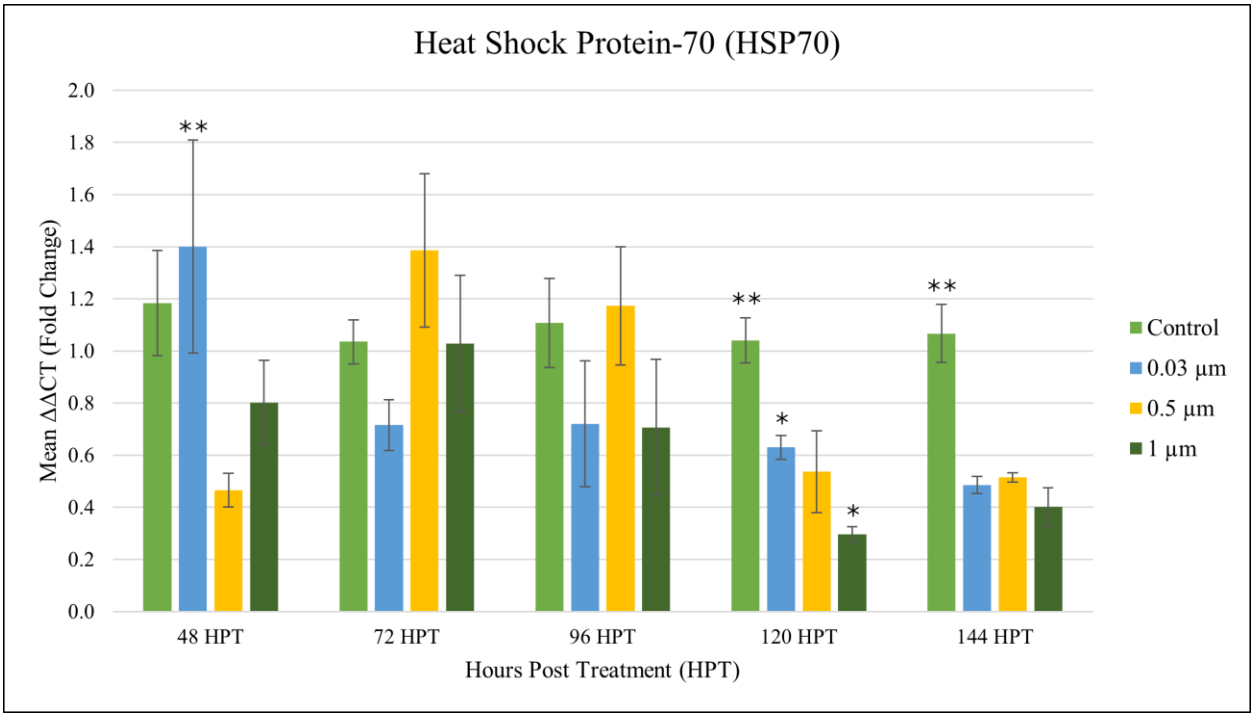

*Figure 13: Heat shock protein-70 (HSP70) relative gene expression changes over 144 hours of exposure to NP treatments (n=4 per treatment). ** Indicates significant fold change value compared to all on treatments in that period. * Indicates significant difference between another treatment.*

difference of 0.4 from 0.03 µm, 0.5 from 0.5 µm, and a 0.7 1.0 µm (p-value <0.05). Also, at 120 HPT, 0.03 µm was significantly upregulated from 1.0 µm with a fold change difference of 0.3 (p-value < 0.05). At 144 HPT, the control was still significantly upregulated with a fold change difference of 0.6 from 0.03 µm and 0.5 µm, and 0.7 from 1.0 µm.

For gene CYP450, results also showed variation in gene expression over development for treatment groups while the control values stayed relatively similar, as seen in Figure 14. At 48 HPT, the 1.0 µm treatment was significantly upregulated with a 1.5- fold change difference from the control, 1.5 from 0.03 µm, and 1.7 from 0.5 µm (p-value <0.05). Then at 96 HPT 0.03 µm treatment was significantly down-regulated by a 0.3 –fold change from control, 0.5 from 0.5 µm, and 1.0 from 1.0 µm (p-value <0.05). At 120 HPT treatment 1.0 µm was significantly down-regulated by 0.5 – fold change from the control, 0.6 from treatment 0.03 µm, and 0.5 from

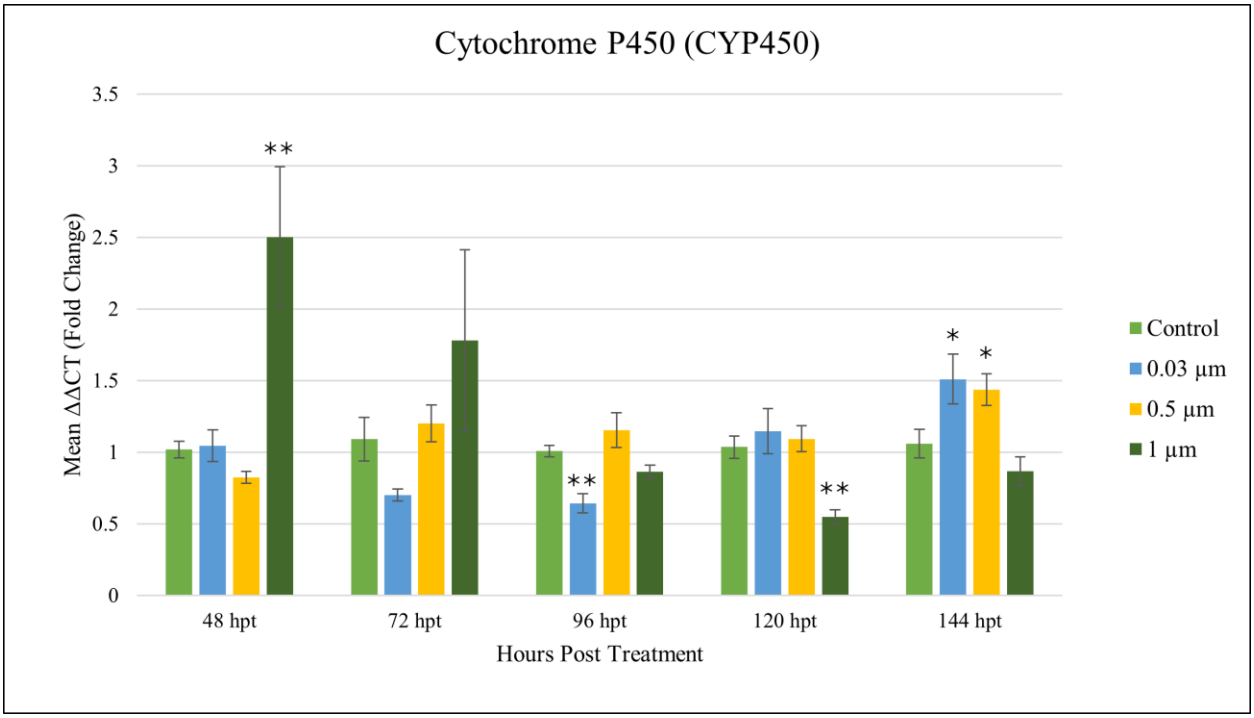

*Figure 14: Cytochrome P450 (CYP450) relative gene expression changes over 144 hours of exposure to NP treatments (n=4 per treatment). ** indicates significant fold change value compared to all on treatments in that period. * Indicates significant difference between another treatment.*

treatment 0.5 µm (p-value <0.05). At 144 HPT, the 0.03 µm was significantly upregulated compared to control by a fold change difference of 0.5. Treatment 0.5 µm was significantly upregulated compared to the 1.0 µm treatment by 0.6- fold change (p-value <0.05).

Gene MIF, which can be seen in Figure 15, was significantly upregulated for control treatment during 96 HPT compared to the rest, with a 0.6 - fold change difference from 0.03 µm, 0.4 from 0.5 µm, and 0.6 from 1.0 µm (p-value <0.05). At 120 HPT, MIF was significantly upregulated for treatment 0.03 µm compared to the rest, with a 1.8 - fold change difference from

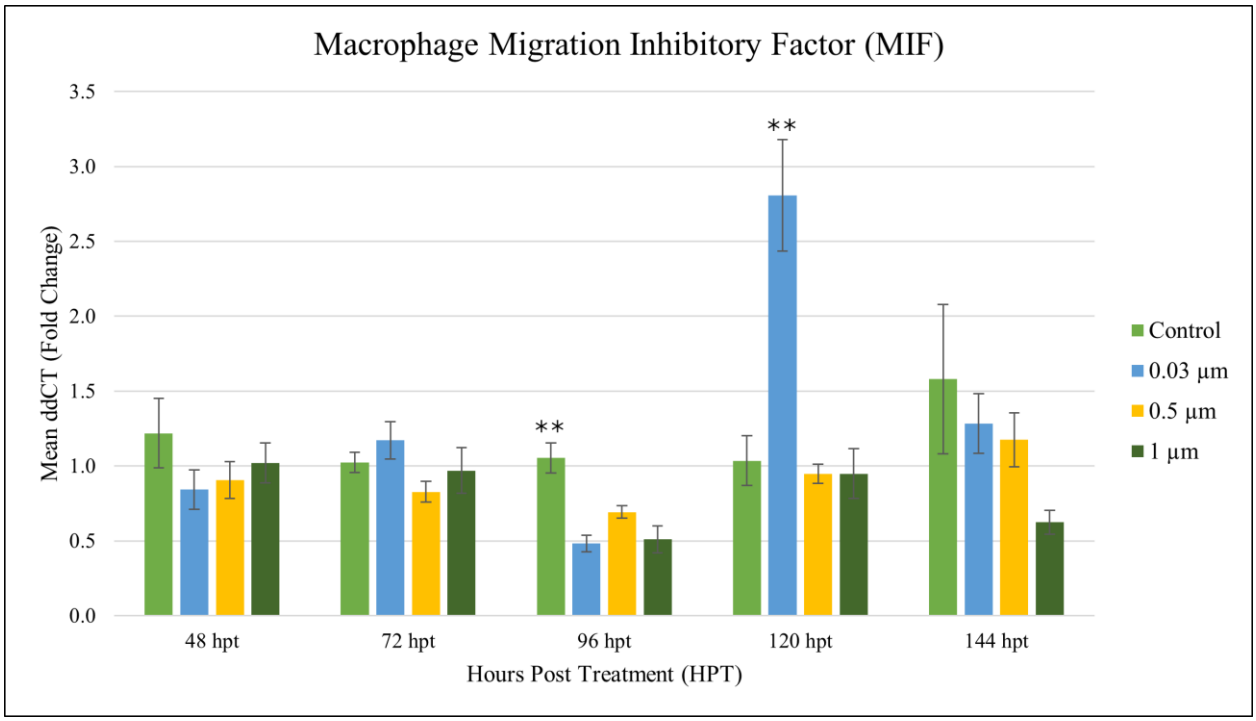

*Figure 15: Macrophage Migration Inhibitory Factor (MIF) relative gene expression changes over 144 hours of exposure to NP treatments (n=4 per treatment). ** indicates significant fold change value compared to all on treatments in that time period. * Indicates significant difference between another treatment.*

control, 1.9 from 0.5 µm, and 1.0 µm (p-value <0.05). Gene MATN1, in Figure 16, had similar significance values compared to gene MIF. During 96 HPT MANT1, the control was significantly upregulated compared to the rest, with a 0.3 - fold change difference from 0.03 µm, 0.4 from 0.5 µm, and 0.2 from 1.0 µm (p-value <0.05). At 120 HPT, MIF was significantly upregulated for

treatment 0.03 µm compared to the rest with a 0.1 - fold change difference from control and significantly down-regulated 0.1 from 0.5 µm and 0.2 from 1.0 µm (p-value <0.05).

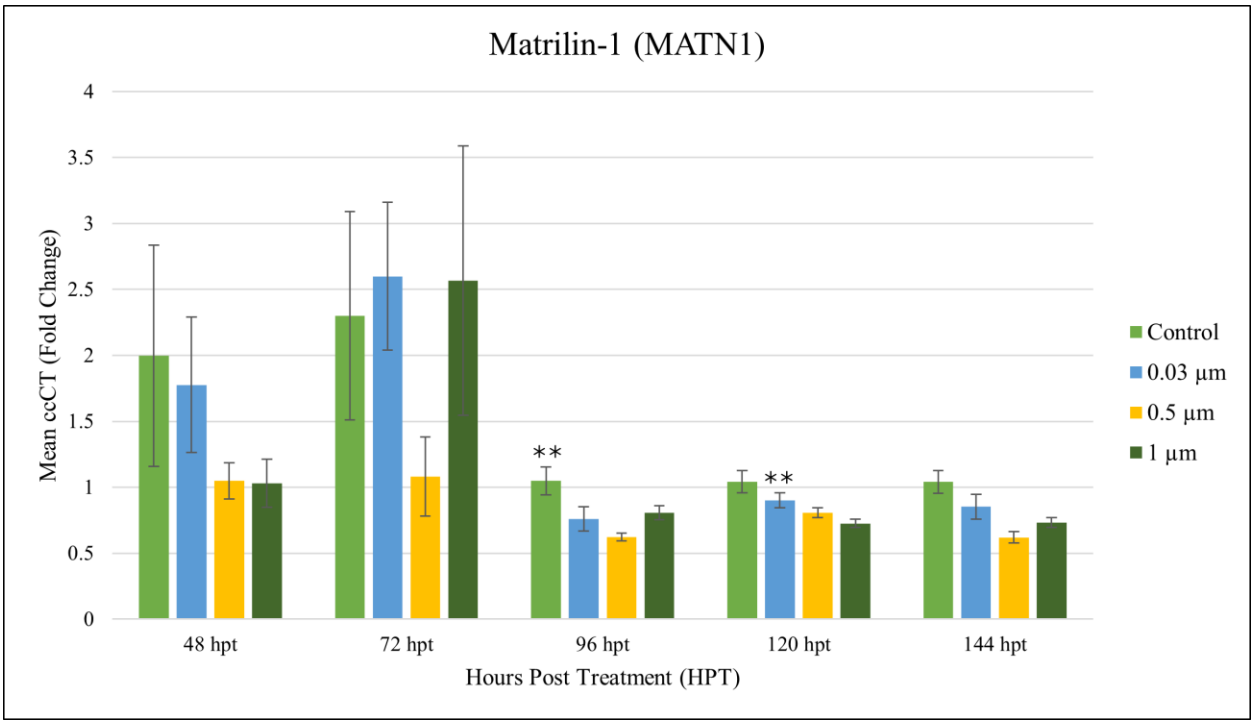

*Figure 16: Cartilage Matrix Protein (MATN1) relative gene expression changes over 144 hours of exposure to NP treatments (n=4 per treatment). ** indicates significant fold change value compared to all on treatments in that period. * Indicates significant difference between another treatment.*

Gene regulation by timepoint of which treatments had significant changes in the up or down-regulation of the respective gene being evaluated can be below in Table 2. The blue upward triangle indicates a significant up-regulation of the gene from the control, and the red downward triangle indicates significant down-regulation from the control. As seen in Table 2, there were no significant changes in gene regulation among any of the genes at 72 HPT. At 120 and 144 HPT, gene HPS70 was down-regulated among all the treatments while it had previously only by significantly upregulated in 48 HPT during treatment 0.03 µm. At 96 and 144, gene MAT was significantly down-regulated among all the treatments. Gene MIF at 96 HPT saw a significant down-regulation among all treatments and then saw an up-regulation at 120 HPT only by treatment

0.03 µm. Gene CYP450 was most affected by treatments 0.03 µm and 1.0 µm. At 48 HPT, CYP450 was upregulated by 1.0, then at 96 HPT was down-regulated by treatment 0.03, at 120 HPT, it was down-regulated by 1.0, and lastly, at 144 HPT, all the treatments induced up-regulation.

Table 2: Relative gene expression results organized by HPT.

HPT	Gene Expression	Treatment	Gene
48	▲	0.03	HSP70
	▲	1.0	CYP450
96	▼	0.03	CYP450
	▼	0.03, 0.5, 1.0	MIF
	▼	0.03, 0.5, 1.0	MAT
120	▲	0.03	MIF
	▼	1.0	CYP450
	▼	0.03, 0.5, 1.0	HSP70
144	▲	0.03, 0.5, 1.0	CYP450
	▼	0.03, 0.5, 1.0	MAT
	▼	0.03, 0.5, 1.0	HSP70

Acute Toxicity Assays

The embryo hatching rate and mortality during exposure to four different treatments, control, 0.03 µm, 0.5 µm, and 1.0 µm NPs, all at 1.0 ppm, were shown in Figures 17 and 18, respectively. Treatment 0.03 µm had a sample size of 109 embryos, 0.5 µm had 124 embryos, 1.0 µm had 107 embryos, and the control had 101 embryos. Hatching rates in Figure 17 showed size-

dependent patterns with later hatching. On the second and fourth day of hatching, embryos in the treatment 1.0 µm had significantly less hatching than in the other treatments ($p < 0.05$). By day two, no embryos had begun hatching, while the other treatments all hatched above 50%. On day

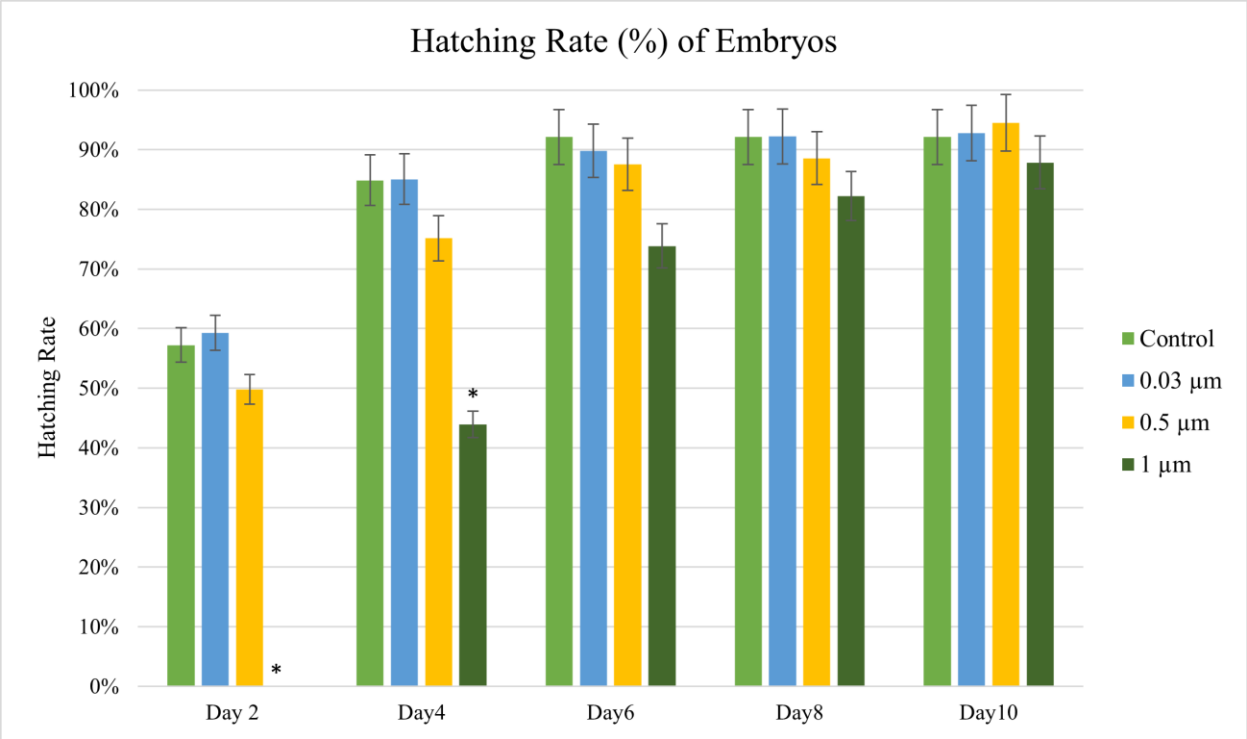

*Figure 17: Hatching Rate (%) of embryos over a period of 10 days after embryonic development. * Signifies significant difference (p-value < 0.05) from other treatments.*

four of hatching, 31% less hatching had occurred compared to treatment 0.05 µm, and 41% less hatching compared to treatments 0.03 µm and the control.

There were no significant differences ($p < 0.05$) identified in embryo mortality rates between the control and any of the treatment groups (Figure 18). The 1.0 µm treatments had the highest mortality rate at 12%, and 0.03 µm treatments had the second highest at 7%. By day six, embryos in the control egg masses had either hatched or were deceased. This was the same for treatment 0.03 µm and 0.5 µm on day 8. On day ten, the last of the unhatched embryos had died. The was such a significant difference in death rates compared between all treatments. Overall

results showed that the 1.0 µm treatment had delayed hatching compared to the other treatments, as well as the highest death rates.

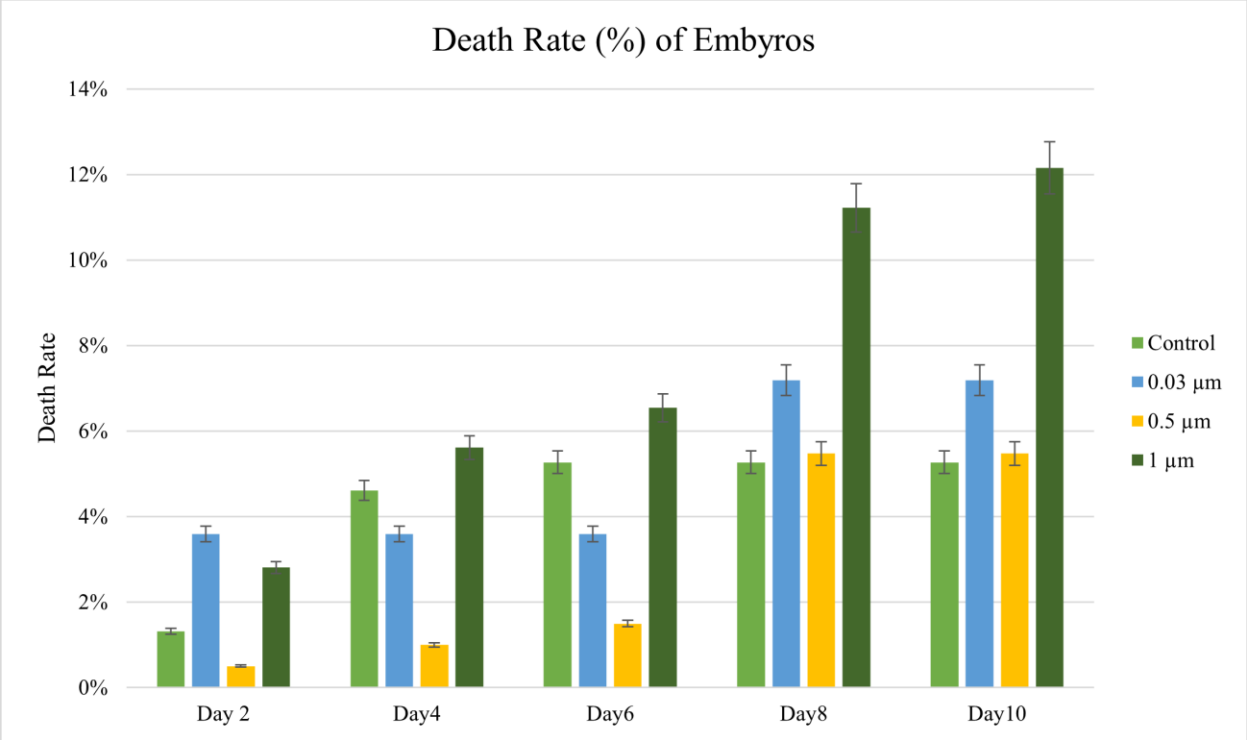

Figure 18: Death Rate (%) of Embryos over 10-day period after embryonic development.

4. DISCUSSION AND CONCLUSION

Nanoplastics in the environment are of increasing concern due to their ability to cross biological membranes and numerous negative effects on the behavior, development, and survival rates of organisms. (Balbi *et al*., 2017; Cui *et al*., 2017; Lee *et al*., 2013; Pitt *et al*., 2018; Sökmen *et al*., 2020). In this study, we investigated the effects of NPs on the embryonic development of *Biomphalaria glabrata*, a commonly used gastropod in toxicology studies. Although the accumulation of NPs with all tested sizes was observed in the *B. glabrata* embryos, the amount of NPs adsorbed by the embryos could not be consistently estimated by the fluorescent plate reader. Reduced fluorescent emissions over exposure time were observed across all three NP treatments. The fluorescent emission results for 0.03 μm had a concentration difference of 0.08 difference ppm compared to the control, which was not supported by fluorescent imaging. Due to the size of the PNPs at an environmentally relevant concentration, 1.0 ppm, the device may not be able to detect the fluorescent signals fully. One paper found that 0.2 μm polystyrene beads were "readily" absorbed by zebra fish embryos which did result in size-dependent observations of fluorescent intensity (Lee *et at*., 2019). Our fluorescent images were inconclusive and were not able to determine if the 0.03 μm was able to penetrate the outer membrane and therefore affect the measurable fluorescent intensity.

Fluorescent images of embryonic masses exposed to fluorescently tagged PNPs showed bioaccumulation of PNPs on the surface of the egg masses across all three treatments. In the first 24 hours of exposure to NPs, the amount of bioaccumulation seemed to be correlated with increasing size. Treatment 0.03 μm had a single florescent signal while the other two treatments had a much greater amount of accumulation, with treatment 1.0 μm having a greater amount than treatment 0.5 μm. Fluorescent images, although qualitative, current data suggest a correlation

between increasing bioaccumulation of PNPs over exposure time, as seen in Figure 7. At 96 HPT, many more NPs can be visualized as well as clusters of NPs which is suggested by the increased diameter of fluorescent signals. While the engineered PNPs used are colloidally stable in snail water, and sinking of PNPs was unlikely to occur, it is known that NPs accumulate in lipid-rich tissues of mussels and fish and are suspected to also absorb to lipid bilayers of membranes (Rossi *et al.*, 2014). This could explain the increased bioaccumulation on the outer membrane over exposure time even while the NPs were not expected to sink during the treatment duration.

While none of the egg masses from the 0.03 μm PNPs at 1.0 ppm produced hatched juveniles with fluorescent signals, a preliminary experiment using egg masses exposed to the 0.03 μm NPs at 10.0 ppm did see a hatched juvenile with what looked like fluorescent NP signals in the shell. This is supported by previous literature, which found bioaccumulation and toxicity are affected by bioavailability and size in calms, copepods, and zebrafish (Lee *et al.*, 2013; Lee *et al.*, 2019; Pan *et al.*, 2012). This may suggest, but does not conclusively determine, that NPs at higher concentrations are capable of being uptaken by embryos during development.

The expression of several stress response genes from *B. glabrata* was tested under the stress of NPs in this study. Heat shock proteins (HSPs), or stress response proteins, are a family of proteins that are over-expressed in response to both abiotic and biotic stimuli. HSP70 is an important protein within the HSP family that aid in an organism's ability to mitigate stress responses and cellular damage from the environment (Srivastava 2002; Song *et al.*, 2014). This gene was chosen as a means to see how PNPs in an aquatic environment could affect an organism's stress and cellular damage due to stressful environments. The only significant up-regulation of gene HSP was 0.03 at 48 HPT, while at 120 HPT, the treatment groups were down-regulated compared to the controls. Thus, the results of this study do not show that 0.03 μm PNPs and 1.0

ppm did not induce a prolonged stress response during embryonic development. HSP70 results of other species showed up-regulation of the stress response when exposed to NP at 1.0 ppm concentrations (Lui *et al*., 2019; Abarghouei *et al*., 2021).

CYP450 is an ancient superfamily of enzymes that plays a prominent role in metabolizing endogenous substances, including vitamins, steroids, fatty acids, and xenobiotics. Because the CYP450s are capable of carrying out a diverse range of monooxygenase activities, it allows for comprehensive protection from an extensive array of xenobiotics that organisms interact with regularly (Simpson 1997). In research, gene expression is used as a bioindicator for PAH contamination in various species, including fish and aquatic invertebrates (Li et at., 2021; Whalen *et al.*, 2010; Chaty *et al.*, 2004). The gene was used to investigate if PNPs would induce a xenobiotic response. At 48 HPT, only the 1.0 μm PNPs showed a significant upregulation compared to the control, but not again during the treatment period. Then not till 144 HPT 0.03 μm and 0.5 μm had significant upregulation. This may indicate that the outer membrane of the egg mass may serve as protection from xenobiotic interaction with the embryos, as it was not until they started to emerge did we see another upregulation of the CYP450 gene. CYP expression in other studies showed upregulation of this gene at doses below 1.0 ppm (Wu *et al*., 2019).

Matrilin genes, or cartilage matrix proteins (CMP), are a protein family associated with the formation of extracellular matrices of different tissues. Specifically, the MATN1 gene used in this study is mainly expressed in cartilage (Deák *et al*., 1999). A matrilin-like protein sequence was identified from *B. glabrata* and is similar to MANT from *Mus musculus (*Bouchut, 2006). Furthermore, Wu *et al*., 2017 found this gene expression during the early development stages of *B. glabrata*. We selected this gene coding for MANT1 as a means of determining if PNPs affect embryonic development. qPCR results yielded no significant upregulation for any of the treatments

over the exposure period compared to the control. This suggests that PNPs at this concentration do not significantly affect the expression of MANT1. No other study was found using this gene to investigate responses to NP pollution.

MIF is widely considered to be a multifunctional protein connected to processes such as cytokine immune responses, cell proliferation, embryonic development, and acute inflammation (Wang *et al.*, 2009). Mitta *et al.*, 2005 identified sequences similar to MIF of vertebrates in *B. glabrata* and then characterized the same function in *B. glabrata's* response to the parasite *S. mansoni* (Garcia *et al*., 2010). MIF was selected for this study as another stress response of embryos when exposed to PNPs. Our results showed a significant upregulation of the MIF gene for treatment of 0.03 μm but otherwise did induce a significant change in gene expression compared to the control. This was consistent with another study's results which found the concentration of NPs, the stronger the down-regulation of MIF (Isabella *et al*., 2019).

Many of the genes selected for this experiment were found from studies regarding parasitology, as relative gene expression has not been studied in *B. glabrata* concerning NP pollution. Not all our results for *B. glabrata* were synonymous with studies of other species, mostly *Daphnia sp*. and fish (Abarghouei *et al*., 2021; Isabella *et al*., 2019; Lui *et al*., 2019; Wu et al., 2019). While gene expression results during embryonic development could not be linked directly to the NPs from absorption to the embryo, the changes in gene expression could be explained by the increased bioaccumulation of NPs on the surface of the egg mass, negatively affecting nutrient and gas exchange to the embryo. Thus the bioaccumulation of NPs on the surface of the egg mass can induce alterations in the relative gene expression of several stress response genes.

No significant differences were identified between treatments of both hatching and mortality rates compared to the control, but hatching rates did show size-dependent patterns with

later hatching. The results of the largest of the PNPs used in this experiment yielded the 1.0 μm treatment had delayed hatching compared to the other treatments as well as the highest death rates. The significance values of our results are not consistent with other studies using *B. glabrata* which found other NP materials such as cuboidal iron ions with diameters of 7.5 ±3.2 nm at 1.0 to 15 ppm (Caixeta *et al*., 2021) and spherical cadmium telluride (CdTe) quantum dots of 3 nm at 1.2nM to 20 nM concentrations (Lima *et at*., 2018) to have significant effects on mortality and hatching delay. Our results did follow similar trends as these studies. It is hypothesized that the bioaccumulation of larger NPs on the surface of the egg mass inhibited the embryo's ability to hatch and ultimately resulted in their death within the egg mass. This would explain the showed size-dependent patterns with later hatching, and the largest NP, 1.0 μm, would have the longest delayed hatching and highest mortality.

In conclusion, we were able to investigate the bioaccumulation of PNPs on the egg mass but did not find evidence of NP pathways to the embryo. Measured genetic responses were altered from the control groups but did not have consistent significant differences in gene expression among the treatments. We expected treatment of 0.03 μm to have the highest morality, but our results showed it was the 1.0 μm treatment that had the highest mortality rates, as well as hatching inhibition.

Invertebrates are a major trophic component within the aquatic and terrestrial environments. Because of their position at the base of their respective ecosystem's food-web(s) and their reproductive rates, invertebrates are a major source of energy to higher trophic organisms. Because of this, they often serve as a bioindicator for the health of an ecosystem (Lagadic & Caquet 1998). The bioaccumulation and hatching inhibition as a result of NP pollution in this study suggest aquatic snails may be at higher risk of toxic NMPs loads and could pose a concern for

biomagnification in an aquatic and terrestrial ecosystem, ultimately polluting human food sources (Lehner *et al.*, 2019). It is advised to further testing be conducted to further study *B. glabrata's* potential as an indicator of ecotoxicology studies.

REFERENCES

Wu, X. J., Dinguirard, N., Sabat, G., Lui, H. Di, Gonzalez, L., Gehring, M., Bickham-Wright, U., & Yoshino, T. P. (2017). Proteomic analysis of Biomphalaria glabrata plasma proteins with binding affinity to those expressed by early developing larval Schistosoma mansoni. *PLoS Pathogens*, *13*(5). https://doi.org/10.1371/journal.ppat.1006081

Lee, W. S., Cho, H. J., Kim, E., Huh, Y. H., Kim, H. J., Kim, B., Kang, T., Lee, J. S., & Jeong, J. (2019). Bioaccumulation of polystyrene nanoplastics and their effect on the toxicity of Au ions in zebrafish embryos. *Nanoscale*, *11*(7). https://doi.org/10.1039/c8nr09321k

Kashiwada, S. (2021). Response to "comment on 'distribution of nanoparticles in the see-through medaka (Oryzias latipes).'" In *Environmental Health Perspectives* (Vol. 129, Issue 12). https://doi.org/10.1289/EHP10585

Isabella, E.-S. E., Pinsino, A., Brugman, S., Barreda, D. R., Torrealba, D., More-Bayona, J. A., & Wakaruk, J. (2019). Innate Immunity Provides Biomarkers of Health for Teleosts Exposed to Nanoparticles. *Frontiers in Immunology | Www.Frontiersin.Org*, *1*, 3074. https://doi.org/10.3389/fimmu.2018.03074

Giusti, A., Leprince, P., Mazzucchelli, G., Thomé, J.-P., & Lagadic, L. (2013). Proteomic Analysis of the Reproductive Organs of the Hermaphroditic Gastropod Lymnaea stagnalis Exposed to Different Endocrine Disrupting Chemicals. *PLoS ONE*, *8*(11), 81086. https://doi.org/10.1371/journal.pone.0081086

Rainieri, S., Conlledo, N., Larsen, B. K., Granby, K., & Barranco, A. (2018). Combined effects of microplastics and chemical contaminants on the organ toxicity of zebrafish (Danio rerio). *Environmental Research*, *162*, 135–143. https://doi.org/10.1016/J.ENVRES.2017.12.019

Tosetto, L., Culum Brown, ·, & Williamson, J. E. (2016). Microplastics on beaches: ingestion and behavioural consequences for beachhoppers. *Marine Biology*, *163*. https://doi.org/10.1007/s00227-016-2973-0

Wu, D., Liu, Z., Cai, M., Jiao, Y., Li, Y., Chen, Q., & Zhao, Y. (2019). Molecular characterisation of cytochrome P450 enzymes in waterflea (Daphnia pulex) and their expression regulation by polystyrene nanoplastics. *Aquatic Toxicology*, *217*, 105350. https://doi.org/10.1016/J.AQUATOX.2019.105350

Wang, B., Zhang, Z., Wang, Y., Zou, Z., Wang, G., Wang, S., Jia, X., & Lin, P. (2009). Molecular cloning and characterization of macrophage migration inhibitory factor from small abalone Haliotis diversicolor supertexta. *Fish & Shellfish Immunology*, *27*(1), 57–64. https://doi.org/10.1016/J.FSI.2009.04.004

Pan, J. F., Buffet, P. E., Poirier, L., Amiard-Triquet, C., Gilliland, D., Joubert, Y., Pilet, P., Guibbolini, M., Risso De Faverney, C., Roméo, M., Valsami-Jones, E., & Mouneyrac, C. (2012). Size dependent bioaccumulation and ecotoxicity of gold nanoparticles in an endobenthic invertebrate: The Tellinid clam Scrobicularia plana. *Environmental Pollution*, *168*, 37–43. https://doi.org/10.1016/J.ENVPOL.2012.03.051

Mitta, G., Galinier, R., Tisseyre, P., Allienne, J. F., Girerd-Chambaz, Y., Guillou, F., Bouchut, A., & Coustau, C. (2005). Gene discovery and expression analysis of immune-relevant genes from Biomphalaria glabrata hemocytes. *Developmental & Comparative Immunology*, *29*(5), 393–407. https://doi.org/10.1016/J.DCI.2004.10.002

Li, L., Ping, X., Li, Z., Xv, G., Wang, C., & Jiang, M. (2021). *Environmental Pollutants and Bioavailability ISSN: (Print) (Online) Journal homepage: https://www.tandfonline.com/loi/tcsb21 Effects of oxidation defense system exposure to*

Benzo(a)pyrene on CYP450 gene expression and EROD activity in Crassostrea gigas and Mytilus coruscus Effects of oxidation defense system exposure to Benzo(a)pyrene on CYP450 gene expression and EROD activity in Crassostrea gigas and Mytilus coruscus. https://doi.org/10.1080/26395940.2021.1952111

Liu, Z., Yu, P., Cai, M., Wu, D., Zhang, M., Huang, Y., & Zhao, Y. (2019). Polystyrene nanoplastic exposure induces immobilization, reproduction, and stress defense in the freshwater cladoceran Daphnia pulex. *Chemosphere*, *215*, 74–81. https://doi.org/10.1016/J.CHEMOSPHERE.2018.09.176

Lee, K.-W., Joon Shim, W., Youn Kwon, O., & Kang, J.-H. (2013). *Size-Dependent Effects of Micro Polystyrene Particles in the Marine Copepod Tigriopus japonicus*. https://doi.org/10.1021/es401932b

Green, D. S., Boots, B., Sigwart, J., Jiang, S., & Rocha, C. (2016). Effects of conventional and biodegradable microplastics on a marine ecosystem engineer (Arenicola marina) and sediment nutrient cycling. *Environmental Pollution*, *208*, 426–434. https://doi.org/10.1016/J.ENVPOL.2015.10.010

Cui, R., Woong Kim, S., & An, Y.-J. (n.d.). *Polystyrene nanoplastics inhibit reproduction and induce abnormal embryonic development in the freshwater crustacean Daphnia galeata OPEN*. https://doi.org/10.1038/s41598-017-12299-2

Deák, F., Wagener, R., Kiss, I., & Paulsson, M. (1999). The matrilins: a novel family of oligomeric extracellular matrix proteins. *Matrix Biology*, *18*(1), 55–64. https://doi.org/10.1016/S0945-053X(98)00006-7

Chaty, S., Rodius, F., & Vasseur, P. (2004). A comparative study of the expression of CYP1A and CYP4 genes in aquatic invertebrate (freshwater mussel, Unio tumidus) and vertebrate

(rainbow trout, Oncorhynchus mykiss). *Aquatic Toxicology*, *69*(1), 81–94. https://doi.org/10.1016/J.AQUATOX.2004.04.011

Caixeta, M. B., Araújo, P. S., Rodrigues, C. C., Gonçalves, B. B., Araújo, O. A., Bevilaqua, G. B., Malafaia, G., Silva, L. D., & Rocha, T. L. (2021). Risk assessment of iron oxide nanoparticles in an aquatic ecosystem: A case study on Biomphalaria glabrata. *Journal of Hazardous Materials*, *401*, 123398. https://doi.org/10.1016/J.JHAZMAT.2020.123398

Bouchut, A., Roger, E., Coustau, C., Gourbal, B., & Mitta, G. (2006). Compatibility in the Biomphalaria glabrata/Echinostoma caproni model: Potential involvement of adhesion genes. *International Journal for Parasitology*, *36*(2), 175–184. https://doi.org/10.1016/J.IJPARA.2005.09.009

Abarghouei, S., Hedayati, A., Raeisi, M., Hadavand, B. S., Rezaei, H., & Abed-Elmdoust, A. (2021). Size-dependent effects of microplastic on uptake, immune system, related gene expression and histopathology of goldfish (Carassius auratus). *Chemosphere*, *276*, 129977. https://doi.org/10.1016/J.CHEMOSPHERE.2021.129977

Hillier, L. W., Jones, C. S., Loker, E. S., Knight, M., Minx, P., Oliveira, G., Raghavan, N., Shedlock, A., Rodrigues do Amaral, L., Arican-Goktas, H. D., Assis, J. G., Hideo Baba, E., Baron, O. L., Bayne, C. J., Bickham-Wright, U., Biggar, K. K., Blouin, M., Bonning, B. C., Botka, C., … Adema, C. M. (2017). Whole genome analysis of a schistosomiasis-transmitting freshwater snail. *Nature Communications*, *8*. https://doi.org/10.1038/ncomms15451

Rossi, G., Barnoud, J., & Monticelli, L. (2014). Polystyrene nanoparticles perturb lipid membranes. *Journal of Physical Chemistry Letters*, *5*(1). https://doi.org/10.1021/jz402234c

Balbi, T., Camisassi, G., Montagna, M., Fabbri, R., Franzellitti, S., Carbone, C., Dawson, K., & Canesi, L. (2017). Impact of cationic polystyrene nanoparticles (PS-NH2) on early embryo development of Mytilus galloprovincialis: Effects on shell formation. *Chemosphere*, *186*. https://doi.org/10.1016/j.chemosphere.2017.07.120

Van Cauwenberghe, L., Vanreusel, A., Mees, J., & Janssen, C. R. (2013). Microplastic pollution in deep-sea sediments. *Environmental Pollution*, *182*. https://doi.org/10.1016/j.envpol.2013.08.013

Lagarde, F., Olivier, O., Zanella, M., Daniel, P., Hiard, S., & Caruso, A. (2016). Microplastic interactions with freshwater microalgae: Hetero-aggregation and changes in plastic density appear strongly dependent on polymer type. *Environmental Pollution*, *215*. https://doi.org/10.1016/j.envpol.2016.05.006

Cole, M., Lindeque, P. K., Fileman, E., Clark, J., Lewis, C., Halsband, C., & Galloway, T. S. (2016). Microplastics Alter the Properties and Sinking Rates of Zooplankton Faecal Pellets. *Environmental Science and Technology*, *50*(6). https://doi.org/10.1021/acs.est.5b05905

Long, M., Moriceau, B., Gallinari, M., Lambert, C., Huvet, A., Raffray, J., & Soudant, P. (2015). Interactions between microplastics and phytoplankton aggregates: Impact on their respective fates. *Marine Chemistry*, *175*. https://doi.org/10.1016/j.marchem.2015.04.003

Murphy, F., Ewins, C., Carbonnier, F., & Quinn, B. (2016). Wastewater Treatment Works (WwTW) as a Source of Microplastics in the Aquatic Environment. *Environmental Science and Technology*, *50*(11). https://doi.org/10.1021/acs.est.5b05416

Browne, M. A., Crump, P., Niven, S. J., Teuten, E., Tonkin, A., Galloway, T., & Thompson, R. (2011). Accumulation of microplastic on shorelines woldwide: Sources and sinks. *Environmental Science and Technology*, *45*(21). https://doi.org/10.1021/es201811s

Besseling, E., Wang, B., Lürling, M., & Koelmans, A. A. (2014). Nanoplastic affects growth of S. obliquus and reproduction of D. magna. *Environmental Science and Technology*, *48*(20). https://doi.org/10.1021/es503001d

Browne, M. A., Dissanayake, A., Galloway, T. S., Lowe, D. M., & Thompson, R. C. (2008). Ingested microscopic plastic translocates to the circulatory system of the mussel, Mytilus edulis (L.). *Environmental Science and Technology*, *42*(13). https://doi.org/10.1021/es800249a

Luo, J., Pei, S., Jing, W., Zou, E., & Wang, L. (2015). Cadmium inhibits molting of the freshwater crab Sinopotamon henanense by reducing the hemolymph ecdysteroid content and the activities of chitinase and N-acetyl-β-glucosaminidase in the epidermis. *Comparative Biochemistry and Physiology Part - C: Toxicology and Pharmacology*, *169*. https://doi.org/10.1016/j.cbpc.2014.10.003

Liu, T., Xing, R., Zhou, Y. F., Zhang, J., Su, Y. Y., Zhang, K. Q., He, Y., Sima, Y. H., & Xu, S. Q. (2014). Hematopoiesis toxicity induced by CdTe quantum dots determined in an invertebrate model organism. *Biomaterials*, *35*(9). https://doi.org/10.1016/j.biomaterials.2013.12.007

Pimentel, D. (1957). Life History of Australorbis Glabratus, The Intermediate Snail Host of Schistosoma Mansoni in Puerto Rico. *Ecology*, *38*(4). https://doi.org/10.2307/1943122

Da Costa, J. P., Nunes, A. R., Santos, P. S. M., Girão, A. V., Duarte, A. C., & Rocha-Santos, T. (2018). Degradation of polyethylene microplastics in seawater: Insights into the environmental degradation of polymers. *Journal of Environmental Science and Health - Part A Toxic/Hazardous Substances and Environmental Engineering*, *53*(9). https://doi.org/10.1080/10934529.2018.1455381

Jambeck, J. R., Geyer, R., Wilcox, C., Siegler, T. R., Perryman, M., Andrady, A., Narayan, R., & Law, K. L. (2015). Plastic waste inputs from land into the ocean. *Science*, *347*(6223). https://doi.org/10.1126/science.1260352

Koelmans, A. A., Besseling, E., & Shim, W. J. (2015). Nanoplastics in the aquatic environment. Critical review. In *Marine Anthropogenic Litter*. https://doi.org/10.1007/978-3-319-16510-3_12

Thomas, J. D., Nwanko, D. I., & Sterry, P. R. (1985). The feeding strategies of juvenile and adult Biomphalaria glabrata (Say) under simulated natural conditions and their relevance to ecological theory and snail control. *Proceedings of the Royal Society of London - Biological Sciences*, *226*(1243). https://doi.org/10.1098/rspb.1985.0090

Bouwmeester, H., Hollman, P. C. H., & Peters, R. J. B. (2015). Potential Health Impact of Environmentally Released Micro- and Nanoplastics in the Human Food Production Chain: Experiences from Nanotoxicology. In *Environmental Science and Technology* (Vol. 49, Issue 15). https://doi.org/10.1021/acs.est.5b01090

Martin, J., Lusher, A., Thompson, R. C., & Morley, A. (2017). The Deposition and Accumulation of Microplastics in Marine Sediments and Bottom Water from the Irish Continental Shelf. *Scientific Reports*, *7*(1). https://doi.org/10.1038/s41598-017-11079-2

Rochman, C. M. (2018). Microplastics research-from sink to source. In *Science* (Vol. 360, Issue 6384). https://doi.org/10.1126/science.aar7734

Maurer-Jones, M. A., Gunsolus, I. L., Murphy, C. J., & Haynes, C. L. (2013). Toxicity of engineered nanoparticles in the environment. *Analytical Chemistry*, *85*(6). https://doi.org/10.1021/ac303636s

Zhang, X. Q., Xu, X., Bertrand, N., Pridgen, E., Swami, A., & Farokhzad, O. C. (2012). Interactions of nanomaterials and biological systems: Implications to personalized nanomedicine. In *Advanced Drug Delivery Reviews* (Vol. 64, Issue 13). https://doi.org/10.1016/j.addr.2012.08.005

Lambert, S., & Wagner, M. (2016). Characterisation of nanoplastics during the degradation of polystyrene. *Chemosphere*, *145*. https://doi.org/10.1016/j.chemosphere.2015.11.078

Eubeler, J. P., Zok, S., Bernhard, M., & Knepper, T. P. (2009). Environmental biodegradation of synthetic polymers I. Test methodologies and procedures. In *TrAC - Trends in Analytical Chemistry* (Vol. 28, Issue 9). https://doi.org/10.1016/j.trac.2009.06.007

Oliveira-Filho, E. C., de Freitas Muniz, D. H., de Carvalho, E. L., Cáceres-Velez, P. R., Fascineli, M. L., Azevedo, R. B., & Grisolia, C. K. (2019). Effects of AgNPs on the snail Biomphalaria glabrata: Survival, reproduction and silver accumulation. *Toxics*, *7*(1). https://doi.org/10.3390/toxics7010012

Oliveira-Filho, E. C., Nakano, E., & Tallarico, L. de F. (2017). Bioassays with freshwater snails Biomphalaria sp.: from control of hosts in public health to alternative tools in ecotoxicology. *Invertebrate Reproduction and Development*, *61*(1). https://doi.org/10.1080/07924259.2016.1276484

Oliveira-Filho, E. C., Geraldino, B. R., Coelho, D. R., De-Carvalho, R. R., & Paumgartten, F. J. R. (2010). Comparative toxicity of Euphorbia milii latex and synthetic molluscicides to Biomphalaria glabrata embryos. *Chemosphere*, *81*(2). https://doi.org/10.1016/j.chemosphere.2010.06.038

De Freitas Tallarico, L. (2015). Freshwater Gastropods as a Tool for Ecotoxicology Assessments in Latin America. *American Malacological Bulletin*, *33*(2). https://doi.org/10.4003/006.033.0220

Oliveira-Filho, E. C., Filho, J. S., Novais, L. A., Peternele, W. S., Azevedo, R. B., & Grisolia, C. K. (2016). Effects of γ-Fe2O3 nanoparticles on the survival and reproduction of Biomphalaria glabrata (Say, 1818) and their elimination from this benthic aquatic snail. *Environmental Science and Pollution Research*, *23*(18), 8362–8368. https://doi.org/10.1007/s11356-016-6998-1

Tallec, K., Huvet, A., Di Poi, C., González-Fernández, C., Lambert, C., Petton, B., Le Goïc, N., Berchel, M., Soudant, P., & Paul-Pont, I. (2018). Nanoplastics impaired oyster free living stages, gametes and embryos. *Environmental Pollution*, *242*. https://doi.org/10.1016/j.envpol.2018.08.020

De Oliveira-Filho, E. C., Matos Lopes, R., & Roma Paumgartten, F. J. (2004). Comparative study on the susceptibility of freshwater species to copper-based pesticides. *Chemosphere*, *56*(4). https://doi.org/10.1016/j.chemosphere.2004.04.026

de Vasconcelos Lima, M., de Andrade Pereira, M. I., Cabral Filho, P. E., Nascimento de Siqueira, W., Milca Fagundes Silva, H. A., de França, E. J., Saegesser Santos, B., Mendonça de Albuquerque Melo, A. M., & Fontes, A. (2019). Studies on Toxicity of Suspensions of CdTe Quantum Dots to Biomphalaria glabrata Mollusks. *Environmental Toxicology and Chemistry*, *38*(10). https://doi.org/10.1002/etc.4525

Toledo, R., & Fried, B. (2011). Biomphalaria snails and larval trematodes. In *Biomphalaria Snails and Larval Trematodes*. https://doi.org/10.1007/978-1-4419-7028-2

Garcia, A. B., Pierce, R. J., Gourbal, B., Werkmeister, E., Colinet, D., Reichhart, J.-M., Dissous, C., & Coustau, C. (n.d.). *Involvement of the Cytokine MIF in the Snail Host Immune Response to the Parasite Schistosoma mansoni*. https://doi.org/10.1371/journal.ppat.1001115

Whalen, K. E., Starczak, V. R., Nelson, D. R., Goldstone, J. V, & Hahn, M. E. (2010). Cytochrome P450 diversity and induction by gorgonian allelochemicals in the marine gastropod Cyphoma gibbosum. In *BMC Ecology* (Vol. 10). https://doi.org/10.1186/1472-6785-10-24

Song, H.-M., Mu, X.-D., Gu, D.-E., Luo, D., Yang, Y.-X., Xu, M., Jian, &, Luo, R., Zhang, J.-E., & Hu, Y.-C. (n.d.). *Molecular characteristics of the HSP70 gene and its differential expression in female and male golden apple snails (Pomacea canaliculata) under temperature stimulation*. https://doi.org/10.1007/s12192-013-0485-0

Sökmen, T. Ö., Sulukan, E., Türkoğlu, M., Baran, A., Özkaraca, M., & Buğrahan Ceyhun, S. (2020). Polystyrene nanoplastics (20 nm) are able to bioaccumulate and causeoxidative DNA damages in the brain tissue of zebrafish embryo (Daniorerio). *Neurotoxicology* , 51–59. https://doi.org/10.1016/j.neuro.2019.12.010

Pitt, J. A., Kozal, J. S., Jayasundara, N., Massarsky, A., Trevisan, R., Geitner, N., Wiesner, M., Levin, E. D., & Di Giulio, R. T. (2018). Uptake, tissue distribution, and toxicity of polystyrene nanoparticles in developing zebrafish (Danio rerio). *Aquatic Toxicology*, *194*, 185–194. https://doi.org/10.1016/j.aquatox.2017.11.017

Kögel, T., Bjorøy, Ø., Toto, B., Bienfait, A. M., & Sanden, M. (2020). Micro- and nanoplastic toxicity on aquatic life: Determining factors. In *Science of the Total Environment* (Vol. 709). https://doi.org/10.1016/j.scitotenv.2019.136050

Lehner, R., Weder, C., Petri-Fink, A., & Rothen-Rutishauser, B. (2019). Emergence of Nanoplastic in the Environment and Possible Impact on Human Health. In *Environmental Science and Technology*. https://doi.org/10.1021/acs.est.8b05512

Chae, Y., & An, Y. J. (2017). Effects of micro- and nanoplastics on aquatic ecosystems: Current research trends and perspectives. *Marine Pollution Bulletin*, *124*(2), 624–632. https://doi.org/10.1016/j.marpolbul.2017.01.070